Wnt5a Evokes Cortical Axon Outgrowth and Repulsive Guidance by Tau Mediated Reorganization of Dynamic Microtubules

Li Li,[1*†] Thomas Fothergill,[2*] B. Ian Hutchins,[1#] Erik W. Dent,[1,2] Katherine Kalil[1,2]

[1] Neuroscience Training Program, University of Wisconsin-Madison, Wisconsin 53706

[2] Department of Neuroscience, University of Wisconsin-Madison, Wisconsin 53706

Received 14 January 2013; revised 24 April 2013; accepted 20 June 2013

ABSTRACT: **Wnt5a guides cortical axons *in vivo* by repulsion and *in vitro* evokes cortical axon outgrowth and repulsion by calcium signaling pathways. Here we examined the role of microtubule (MT) reorganization and dynamics in mediating effects of Wnt5a. Inhibiting MT dynamics with nocodazole and taxol abolished Wnt5a evoked axon outgrowth and repulsion of cultured hamster cortical neurons. EGFP-EB3 labeled dynamic MTs visualized in live cell imaging revealed that growth cone MTs align with the nascent axon. Wnt5a increased axon outgrowth by reorganization of dynamic MTs from a splayed to a bundled array oriented in the direction of axon extension, and Wnt5a gradients induced asymmetric redistribution of dynamic MTs toward the far side of the growth cone. Wnt5a gradients also evoked calcium transients that were highest on the far side of the growth cone. Calcium signaling and the reorganization of dynamic MTs could be linked by tau, a MT associated protein that stabilizes MTs. Tau is phosphorylated at the Ser 262 MT binding site by CaMKII, and is required for Wnt5a induced axon outgrowth and repulsive turning. Phosphorylation of tau at Ser262 is known to detach tau from MTs to increase their dynamics. Using transfection with tau constructs mutated at Ser262, we found that this site is required for the growth and guidance effects of Wnt5a by mediating reorganization of dynamic MTs in cortical growth cones. Moreover, CaMKII inhibition also prevents MT reorganization required for Wnt5a induced axon outgrowth, thus linking Wnt/calcium signaling to tau mediated MT reorganization during growth cone behaviors.** Develop Neurobiol 74: 797–817, 2014

Keywords: **Wnt5a; axon growth and guidance; microtubules; tau; calcium signaling**

INTRODUCTION

Wnts are morphogens that can function as axon guidance cues (Salinas and Zou, 2008; Clark et al., 2012; Salinas, 2012). Wnt5a, *in vivo,* acts as a repulsive guidance cue for cortical axons (Liu et al., 2005). *In vitro* (Li et al., 2009), and in living cortical slices (Hutchins and Kalil, 2011). Wnt5a increases rates of cortical axon outgrowth and induces repulsive axon guidance. Growth cone behaviors are regulated by

Additional Supporting Information may be found in the online version of this article.

*These authors contributed equally to this work.

[†]*Present address:* Galenea, Inc. Wakefield, MA 01880.

[#]*Present address:* National Institute of Neurological Disorders and Stroke, National Institutes of Health, 35 Convent Dr., Bethesda MD, 20892.

Correspondence to: K. Kalil (kakalil@facstaff.wisc.edu).

Contract grant sponsor: National Institutes of Health; contract grant number: NS014428 and GM801642.

Contract grant sponsor: Herman Shapiro fellowship.

Contract grant sponsor: University of Wisconsin Graduate School.

Published online 2 July 2013 in Wiley Online Library (wileyonlinelibrary.com).
DOI 10.1002/dneu.22102

reorganization and dynamics of the actin and microtubule (MT) cytoskeleton (Dent and Gertler, 2003; Lowery and VanVactor, 2009; Dent et al., 2011; Vitriol and Zheng, 2012), which can be modulated by extracellular guidance cues (Song and Poo, 1999; Luo, 2002; Huber et al., 2003; Govek et al., 2005; Kalil and Dent, 2005). Stable MTs occupy the growth cone center, while dynamic MTs that grow and shrink during "dynamic instability" actively explore the periphery (Dent et al., 1999; Dent and Kalil, 2001; Schaefer et al., 2002, 2008; Lowery and Van Vactor, 2009). Inhibiting MT dynamics can abolish growth cone turning and localized MT stabilization and de-stabilization can induce attractive and repulsive turning (Buck and Zheng, 2002), suggesting an instructive role for MTs. Wnt signaling can also promote MT stability through a transcription-independent branch of the canonical β-catenin pathway (Krylova et al., 2000), in which inhibition of GSK-3β decreases MAP-1B phosphorylation (Ciani et al., 2004). During remodeling of DRG (Krylova et al., 2002) and cerebellar mossy fiber terminals (Lucas and Salinas, 1997; Hall et al., 2000) Wnt3a and Wnt7a, respectively, decrease axon length and increase growth cone size by reorganizing the MT cytoskeleton into stable loops (Ciani and Salinas, 2005) through loss of MT directionality (Purro et al., 2008; Budnik and Salinas, 2011). In contrast, Wnt5a increases cortical axon outgrowth and induces growth cone repulsion (Li et al., 2009). However, the cytoskeletal mechanisms regulating these processes are unknown.

Calcium is an essential second messenger that transduces axon guidance signals to regulate growth cone extension and steering (Henley and Poo, 2004; Gomez and Zheng, 2006; Wen and Zheng, 2006; Zheng and Poo, 2007; Tojima et al., 2011). In cortical growth cones, Wnt5a evokes repetitive Ca^{2+} transients, which are required for Wnt5a evoked axon outgrowth and repulsion (Li et al., 2009). CaMKII, downstream of calcium (Hudmon and Schulman, 2002) is required for Wnt5a induced cortical axon outgrowth and guidance (Li et al., 2009; Hutchins and Kalil, 2011). CaMKII phosphorylates the MT associated protein (MAP) tau (Litersky et al., 1996) thereby detaching it from MTs to increase MT dynamics (Biernat et al., 1993). Thus, Wnts can regulate MT organization and dynamics through calcium signaling pathways. In this study, we used high-resolution live cell imaging to investigate how Wnt5a signaling can promote axon growth and guidance by regulating MTs. We found that in response to Wnt5a dynamic MTs in the growth cone reorganized from a splayed, to a bundled array of MTs that reoriented toward the leading edge in the direction of axon extension. In Wnt5a gradients dynamic MTs redistributed to the far side of the growth cone, which coincided with an asymmetry in calcium transients. We hypothesized that tau might link Wnt/calcium signaling to MT reorganization, and found that tau, when phosphorylated within its MT binding site at Ser262, is required for the growth and repulsive guidance effects of Wnt5a by mediating the reorganization of dynamic MTs in the growth cone.

METHODS

Experimental Reagents

The following chemical inhibitors and recombinant protein were used: recombinant human/mouse Wnt5a (R&D systems), Nocodazole (Sigma), Taxol (Sigma). Plasmid constructs used to transfect neuronal cultures included EB3-EGFP (a gift from Dr. Niels Galjart**,** Erasmus University, The Netherlands), DsRed2 (Clontech), Fluo4-momo (Sigma), tau S262A (a gift from Dr. Koichi Iijima and Kanae Iijima-Ando, Thomas Jefferson University), and CaMKIIN-EGFP (a gift from Dr. Thomas Soderling). EB3-tdTomato was created by replacing the EGFP in EB3-EGFP with tdTomato cut from the tdTomato-N1 vector (Clontech) and used in experiments with cotransfected with CaMKIIN-EGFP. Antibodies used for immunocytochemistry included: rat anti-tyrosinated tubulin (Millipore), mouse anti-total tau (tau 46; Cell Signaling Technology), rabbit anti-phospho tau Ser262 (Millipore), Cy2-conjugated donkey anti-rabbit IgG (Jackson ImmunoResearch), Cy2-conjugated donkey anti-rat IgG (Jackson Immuno Research), and Cy5-conjugated donkey anti-mouse IgG (Jackson ImmunoResearch).

Dissociated Cell Culture and Transfection

Dissociated cultures were prepared as previously described (Li et al., 2009). Briefly, cultures were prepared from sensorimotor cortex obtained from postnatal day 0 (P0)-P2 golden Syrian hamsters (*Mesocricetus auratus*) of either sex as described previously (Dent and Kalil, 2003). Electroporation was carried out with a Nucleofector (Amaxa) and Mouse Neurons Kit (Amaxa) according to the recommended protocol. Cotransfection efficiency was tested by transfecting GFP and RFP at the same time. Over 60% of neurons cultured for 2 days expressed GFP while cotransfection efficiency was about 90%. Dissociated primary neurons were plated onto coverslips coated with 0.5 mg/mL poly-D-Lysine (Sigma) and 20 μg/mL laminin (Sigma) at a density of 2–5 K/cm^2 and were incubated in 5% CO_2 and 9% O_2 at 37°C. In some experiments, etched coverslips (Bellco) were used to provide landmarks for locating neurons. Neurons in our cultures have already developed

dendrites and a long axon with a growth cone at 15 h after plating (Szebenyi et al., 1998). Thus, we applied various regents to the medium 1–2 days after plating for the long-term outgrowth assay (4–5 days) and cultures were incubated for an additional 72 h. For short-term outgrowth assays, neurons were dissociated, transfected with plasmid constructs and maintained in culture for 2 days before acute treatments over the course of 1 h.

Measurements of Axon Outgrowth

Measurements of axon outgrowth in the long-term (4–5 days) and short-term (1 h) outgrowth assays were carried out on phase and fluorescence images of neurons, which were acquired with a 20× 0.5 numerical aperture (NA) Plan Fluor objective mounted on a Nikon TE300 Quantum inverted microscope equipped with a Photometrics Cascade II: 512. Only stage 2–3 neurons with pyramidal morphologies and with a clearly identifiable axonal process, more than 100 μm were chosen for analysis. Such neurons are likely to be cortical projection neurons. Axon lengths were measured with the morphometric analysis tools of Metamorph (Molecular Devices) from the cell body to the distal extent of the central region of the growth cone. An axon was defined as a process that remains parallel to the initial axon segment extending from the cell body. Data were saved in Excel 2007(Microsoft) and GraphPad Prism (GraphPad) was used to perform statistical analysis and create graphs. Measurements are given in mean ± SEM unless otherwise noted.

Turning Assays

Glass pipette turning assays, similar to turning assays performed on Xenopus spinal axons (Lohof et al., 1992; Zheng et al., 1994), were carried out on neurons (P2, 2–3 days *in vitro*) with a straight 20 μm segment at the end of the axon. Serum-free medium was replaced by Leibovitz-15 (L15) medium (Gibco) immediately before experiments and pharmacological reagents were added to the medium 30 min before the turning assays. A pipette with a 1 μm tip diameter was filled with Wnt5a (10 μg/mL). The pipette was positioned 100 μm away from the axonal growth cone at a 45° angle from the original direction of axon outgrowth, which was defined by the direction of the 20 μm axon segment; 2 Hz pulses (3psi, 20ms) were generated with a pulse generator (Grass Product Group, SD9) and a Picospritzer II (General Valve). Gradients were confirmed by using fluorescent dextran in place of active protein (data not shown). Phase images of live cells were acquired at 1 min intervals to record growth cone behaviors. Outgrowth rates were quantified by tracing trajectories of the part of the axon that grew out during the 1 h time period. Turning angles were defined as the angles between the original direction of axon outgrowth and a line connecting the original position of the growth cone and its final position. To display axon trajectories, traces of individual axons were made from the final image of each axon at the end of the 1 h turning assay.

Dunn chamber axon guidance assays (Yam et al., 2009) were performed by growing P0 hamster cortical neurons on appropriately coated (see above) 22 mm^2 square #1.5 coverslips (Corning) at a low density (10 k) cells/well in a 6 well plate (Falcon). Assembly of the Dunn chamber (Hawksley, UK) was similar to that in a previous study (Yam et al., 2009). Briefly, Dunn chambers were rinsed once and then filled with serum-free medium. To secure coverslips with neurons on the chamber, sealant (Dow Corning) was applied ~5 mm from the border of the outer well but omitted at one side to form a slit for draining and refilling the outer well. A coverslip with neurons was inverted over the Dunn chamber leaving a narrow slit at the edge without the sealant. Media at the outer well was drained by using a vacuum and then medium with 400 ng/mL Wnt5a was added to the outer well. The narrow slit was sealed by fixing a small piece of parafilm to the chamber with sealant. Images were acquired immediately after Dunn chamber assembly and 2 h later with a 20 × 0.5 NA Plan Fluor objective mounted on a Nikon TE300 Quantum inverted microscope equipped with a Photometrics Cascade II: 512. Due to the requirement of #1.5 coverslips to prevent distortion of the gradient in the Dunn chamber, high-resolution phase images could not be obtained using our objective; however, axonal processes and growth cones could easily be defined in all cases. All dissociated neurons in the bridge region of the Dunn chamber were imaged in each experiment. Dunn chambers were kept at 37°C during imaging. For data analysis, we only included individual axons with >10 μm straight distal end and with net outgrowth > 5 μm/h. The outgrowth of axons was measured by tracing axons from the original position of growth cones to their final position. The original direction of axon outgrowth was defined by the direction of the 10 μm distal axon segment. The initial angle (0–180°) was defined by the angle between the original direction of axon outgrowth and the direction of the Wnt5a gradient. Final angles were calculated as the angles between the original direction of axon outgrowth and a line connecting the original position of the growth cone and its final position. When axons turned towards the gradient, the turning angle was assigned a positive value and when axons turned away from the gradient, the turning angle was assigned a negative value. Images presented in figures were rotated to so that the gradient increases along the y-axis to more easily compare responses of axons.

Immunocytochemistry

At 120 min after exposure to BSA or Wnt5a gradients, or at 60 min after addition of BSA or Wnt5a into the medium, cortical neurons at 2-3DIV were fixed and immunostained as described previously (Dent and Kalil, 2001). Briefly, neurons were fixed with 4% paraformaldehyde (Electron Microscopy Sciences) in Kreb's buffer (pH = 7.4), blocked

by using 10% BSA (Sigma), incubated with diluted primary antibodies (1:100 anti-tyrosinated tubulin, 1:500 anti-Phospho-tau at Ser262 or 1:500 anti-total tau) at 4°C overnight and then incubated with diluted secondary antibodies (1:200 Cy2-conjugated donkey anti-rat IgG, 1:200 Cy2-conjugated donkey anti-rabbit IgG or 1:200 Cy5-conjugated donkey anti-mouse IgG) at room temperature for 1 h. Fluorescence images were acquired with a 60× 1.40 NA Plan Apo objective mounted on the Nikon microscope (tau phosphorylation) or an Olympus (Center Valley) Fluoview 500 laser-confocal system mounted on an AX-70 upright microscope with a 40× plan fluor water immersion objective (tyrosinated tubuin) on the same day and under the same conditions, including exposure time and illumination. To visualize the distribution of dynamic MTs, a threshold of 50% was applied to the tyrosinated-tubulin image, highlighting the top 50% of intensities in green. To quantify distribution of dynamic MTs in growth cones, each growth cone was bisected with a line parallel with the axon shaft, and the ratio of MT fluorescence at the far versus near side was calculated. A ratio above 1 indicates more MTs on the far side than on the near side and a ratio of 1 means no asymmetry. Average fluorescence intensity at Pi-tau and total tau channels in growth cones were measured to calculate ratios of Pi-tau versus total tau. Distribution of Pi-tau and total tau along axons was measured by drawing a one-pixel wide line from axon shafts to growth cones. The length of the line along axon shafts was equal to that along growth cones.

Measurements of Calcium Activity

Calcium measurements and analysis were adapted from Hutchins and Kalil (2008) and Li et al. (2009). For experiments to image calcium transients, cortical neurons grown on poly-D-lysine were loaded with a membrane bound calcium indicator, Fluo 4 MOMO (Sigma, 4 μM) for 20 min. Axons tipped with large growth cones were selected for imaging, since asymmetries in calcium activity are more easily distinguished in large growth cones. Baseline calcium activity was measured for 5 min prior to application of Wnt5a. Images were acquired every 5 s on a Nikon TE300 microscope with 60 × 1.4 NA Plan Fluor objective with a Photometrics Cascade II:512 cooled CCD camera. A pipette containing 10 μg/mL Wnt5a was then positioned 50 μm away from the growth cone at 45° and Wnt5a was ejected from the pipette at 3 PSI twice a second during calcium imaging periods lasting up to 20 min. Neurons expressing spontaneous calcium transients during the control period were excluded from analysis. Otherwise, the fluorescence signal from Fluo 4 MOMO (F) during application of Wnt5a was normalized to the averaged fluorescence signal from the control period (F0). These normalized images (F/F0) were median pass filtered to eliminate single pixel noise. Any calcium signal larger than 3.6 μm^2 and exceeding 135% of baseline was counted as a calcium transient. To quantify the localization of these calcium transients, we measured the center of intensity of calcium transients in MetaMorph and measured the displacement of the center of intensity from the midline of the growth cone (negative displacements were on the side of the growth cone facing away from the pipette).

Live-Cell Imaging with TIRF (Total Internal Reflection Fluorescence Microscopy) and Quantitative Analysis of EB3 Comets

A TIRF microscope consisting of a Nikon TE2000E base with TIRF laser illuminator (Nikon), a Nikon 100×/1.49 NA Plan Apo TIRF objective, a Nikon perfect focus system for continuous automatic focusing of the sample during time-lapse imaging, a motorized x–y stage (Prior Scientific), and a Coolsnap HQ cooled interline CCD camera (Photometrics) was used to image neurons during application of Wnt5a for periods of up to 1 h. For TIRF illumination two lasers were used: a 40 mW Argon laser for EGFP excitation and a 10 mW solid state 561 nM laser for DsRed2 and tdTomato excitation (both Melles-Griot). During time-lapse microscopy, neurons were kept at 37°C with in an incubation chamber (Solent) custom fitted to the microscope and CO_2 diffusion from the media was limited by sealing cultures in a glass-ring chamber with silicone grease. To record baseline dynamics of EB3 movement, fluorescent images of live cells were acquired at 5 s intervals for 30 min before treatment. Wnt5a (400 μg/mL) was then applied to the chamber and resealed before immediately resuming imaging for a further 30 min. All images were collected and compiled with MetaMorph imaging software (Molecular Devices). Basic unsharp mask and low-pass filters were applied to make it easier to identify distinct EB3 comets. ImageJ software (NIH) using the MTrackJ plugin (Dr. Erik Meijering) was used to manually track all EB3 comets throughout both 30 min imaging periods sampled for each growth cone. Binary tracings of comet tracks were then compiled into movies using MTrackJ and imported to Metamorph for further analysis. To determine a measure of MT "clustering," sum total image projections of the binary track movies were first created for the before and during Wnt5a-treatment periods for each growth cone. Pseudocolored representations were made after scaling the two images equally. The Metamorph line-scan feature with a pixel-width of 200 was then used to bin all the pixel intensities in the image across a perpendicular line drawn through the geometric center of the growth cone. A Gaussian distribution curve of the pixel intensities was generated, of which the peak represents the center of maximum intensity within the growth cone and area beneath the curve the standard deviation. As such, a reduction in the standard deviation of this Gaussian curve represents a direct measure of an increase in the amount of MT clustering as measured by overlapping MT tracks. Increases in overlap of the MT tracks result in steeper Gaussian curves.

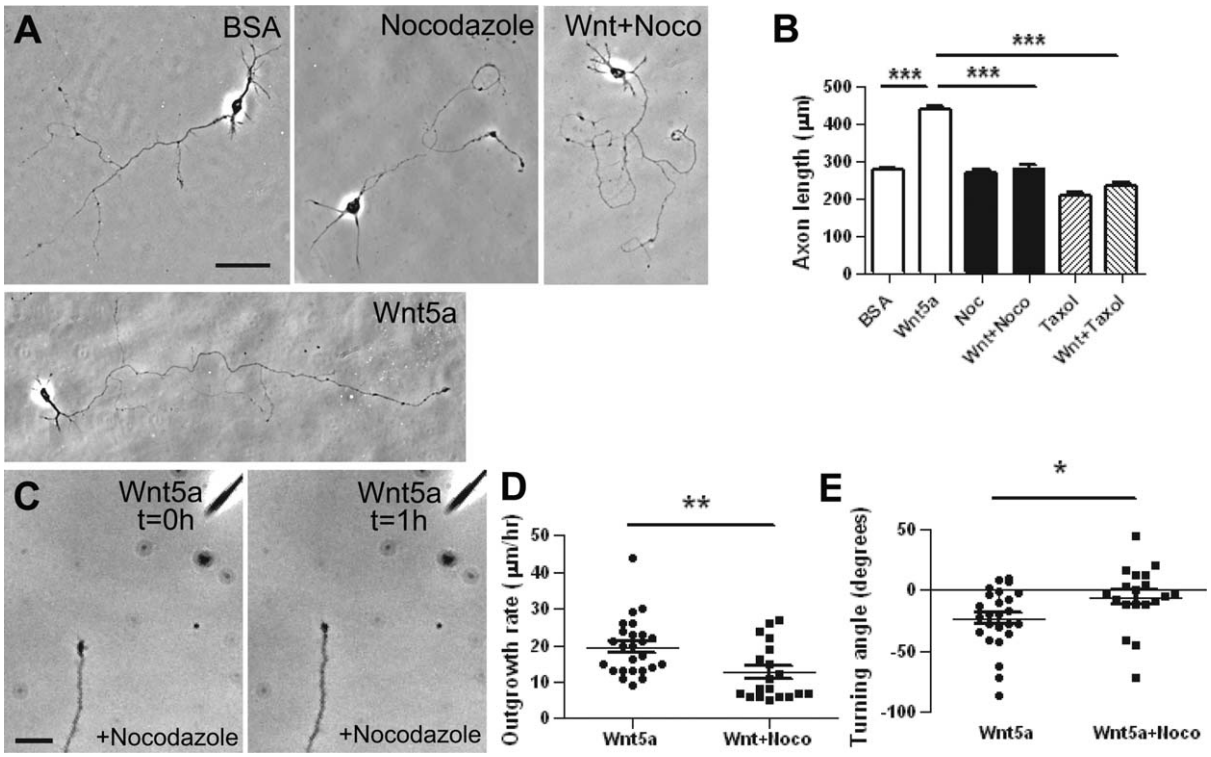

Figure 1 Dynamic MTs are required for Wnt5a induced axon outgrowth and repulsion. A: Representative images of neurons treated with BSA (control), 400 ng/mL Wnt5a, 33 n*M* Nocodazole or Wnt5a, and Nocodazole for 3 days. Treatments were bath applied to neurons 24 h after plating. Scale bar: 50 μm. B: Bar graphs demonstrating the average axon length in different conditions. Wnt5a-promoted axon outgrowth is blocked by inhibiting MT dynamics (33 n*M* Nocodazole or 10 n*M* Taxol). The numbers of cells examined for each condition were over 90. ***$p < 0.001$ (One-way ANOVA followed by Dunnett's post test). C: Images of a cortical axon and its growth cone at the beginning and end of a 1 h exposure to a Wnt5a gradient in the presence of 5–10 n*M* Nocodazole. The Wnt5a gradient failed to repel the axon in the presence of 5–10 n*M* Nocodazole. Scale bar: 20 μm. D, E: Inhibiting MT dynamics (Nocodazole) prevented Wnt5a induced axon outgrowth (D) and repulsive turning (E). Number of axons = 25, 19 in Wnt5a or Wnt5a+Nocodazole treated groups. **$p < 0.01$; *$p < 0.05$ (Mann-Whitney test).

RESULTS

Dynamic MTs Are Required for Wnt5a Evoked Axon Outgrowth and Repulsion

Previously, we found that bath applied Wnt5a increases cortical axon outgrowth and that Wnt5a gradients evoke repulsive growth cone turning away from the Wnt5a source simultaneous with increased outgrowth rates (Li et al., 2009). To investigate the role of MT dynamics and reorganization in these axon behaviors we first investigated whether dynamic MTs are required for the growth promoting and guidance effects of Wnt5a (Fig. 1). We used neurons from P2 hamster sensorimotor cortex, when cortical axons are entering the spinal cord (Reh and Kalil, 1981), and corpus callosum (Norris and Kalil, 1992) where, as shown in mouse (Liu et al., 2005; Keeble et al., 2006), they would encounter Wnt5a gradients. In long-term 4-day experiments, Wnt5a was bath applied to dissociated cortical cultures in the presence of 33 n*M* nocodazole, which inhibits MT dynamics at nanomolar concentrations (Vasquez et al., 1997; Mikhailov and Gundersen, 1998; Dent and Kalil, 2001). To minimize effects on neuronal polarity, Wnt5a or nocodazole was added to the cultures 24 h after plating when axons and dendrites are established. Consistent with our previous results, the average axon length increased from 298.5 ± 8.8 μm in BSA control experiments (n = 260 axons from three separate experiments) to 467.4 ± 12.5 μm (n = 218 axons from three separate experiments) in cultures treated with 400 ng/mL Wnt5a [Fig. 1(A,B)]. Cultures treated with nocodazole failed to show

Wnt5a induced increases in axon outgrowth ($n = 131$ axons from three separate experiments) which averaged 281.5 ± 9.3 μm. However, nocodazole had no effect on cortical axon outgrowth *per se,* which averaged 270.6 ± 8.6 μm ($n = 112$ axons from three separate experiments, Fig. 1B). We also treated cultures with 10 n*M* Taxol, which normally stabilizes MTs but at low nanomolar concentration acts to inhibit MT dynamics. This treatment also prevented increased axon outgrowth by Wnt5a. Axon length averaged 235.2 ± 7.8 μm ($n = 96$ in three separate experiments). Wnt5a applied as a gradient from a pipette increased axon outgrowth rates (averaging 20 μm/h) and induced repulsive axon turning away from the Wnt5a source (average turning angle –23°, $n = 25$ axons) as previously described (Li et al., 2009). In contrast, nocodazole treatment prevented the growth (average growth rate = 13 μm/h) and guidance effects of Wnt5a (average turning angle –5°, $n = 19$ axons, Fig. 1(C–E). These results suggest that MT dynamics are essential for Wnt5a mediated axon outgrowth and guidance.

Dynamic MTs Orient Toward Spontaneous Axon Outgrowth From The Growth Cone

Although previous studies have shown that MTs are required for axon outgrowth (Tanaka et al., 1995) and turning behaviors (Tanaka and Kirschner, 1995; Buck and Zheng, 2002) few studies of mammalian growth cones responding to growth and guidance cues have visualized changes in MT organization with high resolution live cell imaging (Kalil and Dent, 2005; Dent et al., 2011). We first examined the reorganization of dynamic MTs in cortical growth cones undergoing spontaneous axon outgrowth. EB3 is a +TIP protein that binds to the growing plus ends of MTs (Nakagawa et al., 2000). To image MT dynamics (Stepanova et al., 2003) early postnatal cortical neurons were transfected with an EGFP-EB3 construct along with a DsRed2 construct to label the growth cone cytoplasm. We used TIRF (total internal reflection fluorescence) microscopy, which permits better resolution and less photo damage to live cells than wide field microscopy. We imaged EGFP-EB3 comets in motile growth cones in five independent experiments acquiring images every 3 s for periods up to 1 h without deleterious effects on growth cone motility or attenuation of fluorescence. This made it possible to correlate changes in the organization of dynamic MTs with the behavior of the growth cone. As shown in Figure 2 and Supporting Information Movie 1, EGFP-EB3 comets initially explored the entire growth cone randomly in all directions. However, beginning at about 12 min MTs began to reorient in the direction of incipient axon outgrowth from the growth cone. Within one min [Fig. 2(A), frames 12:44–12:59] EGFP-EB3 comets changed their random orientation to align with and invade the nascent axon (arrows). We analyzed the orientation of growing MTs with respect to the direction of spontaneous axon outgrowth by tracing individually all EB3 comets in Metamorph ($n = 608$ comets in this growth cone during the 30 min imaging period). As shown in Figure 2(B), orientation of EB3 comets in the growth cone shown in the movie [Fig. 2(A)] was expressed as an angle between MT orientation and orientation of the growing axon. Over time, the average of these angles became significantly smaller as MTs became aligned with the direction of the developing axon. For example in the first 5 min, the orientation of EB3 comets had an average angle with the nascent axon of 41.5 ± 3.9°. However, in the last 5 min of this imaging sequence the average angle was 18.1 ± 1.9°. This alignment, which occurred by 13 min, was correlated with an axon outgrowth rate that tripled in 20 min after this time point [Fig. 2(C)]. To determine whether more rapid movements of EB3 comets accompanied increased axon outgrowth, we measured rates of comet movement before and after their alignment. We found that before alignment comet velocity was 3.8 ± 0.1 μm/min ($n = 293$ comets) versus 2.9 ± 0.1 μm/min ($n = 315$ comets) after alignment, suggesting that increases in axon outgrowth were correlated with changes in orientation of EB3 comets rather than with increased velocity of EB3 comets.

To determine whether invasion of EB3 comets was instructive or permissive for increased axon outgrowth we compiled kymographs to compare the timing of EB3 invasion with protrusion of the growth cone membrane to form the nascent axon. For each frame, a maximum pixel value was obtained from a three pixel wide line drawn parallel to the long axis of the axonal protrusion from the growth cone [Fig. 2(D)]. These lines from each of 601 frames were arranged horizontally to show protrusive activity of the membrane over time. Protrusion of the DsRed2 labeled cytoplasm (white arrowheads) is shown in red on the y-axis to indicate distance. Similar methods were used to compile kymographs of EB3 comets in green in the same time frame. As shown in Figure 2(D), EB3 comets did not begin to align with and invade the nascent axon until ~13 min (white arrow) shortly before persistent protrusion of the membrane occurred (white arrowheads). This kymographic analysis shows that invasion of EB3 comets into the

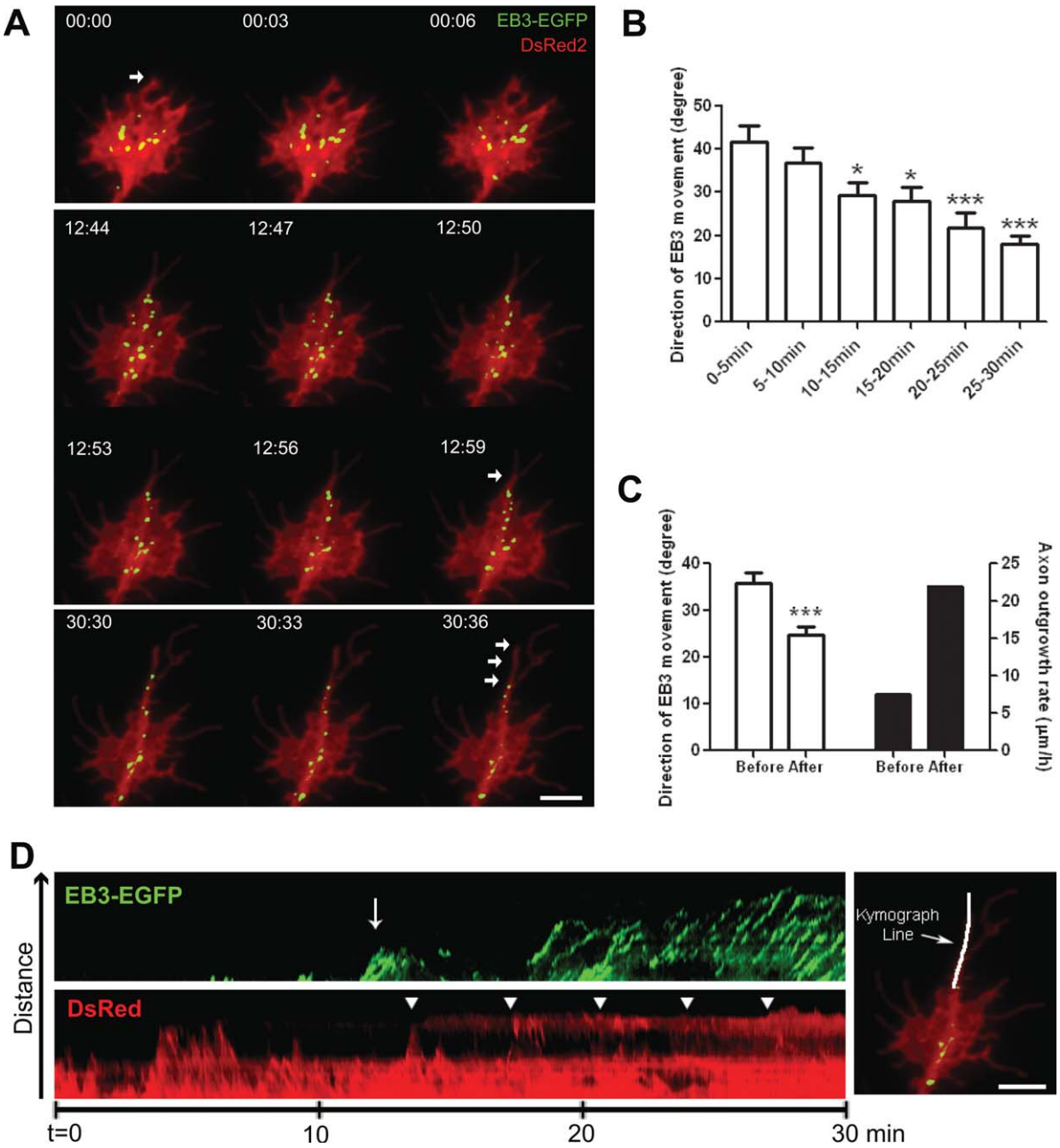

Figure 2 MT reorientation predicts the direction of axon outgrowth. A: Time lapse images acquired in TIRF microscopy showing that EB3 comets (green) randomly explore all regions of the growth cone (labeled by DsRed2 in red) at the beginning of the sequence (top). Subsequently, EB3 comets reorient to align with the axis of future axon outgrowth (middle and bottom). White arrows point to axon protrusion from the growth cone. Time is in minute:second. Scale bar: 5 μm. B: Over time more EB3 comets move in the direction of axon outgrowth (number of comets = 114, 109, 122, 98, 82, 83 in different time windows). Direction of EB3 movement is defined as the angle between EB3 movement and direction of growth cone protrusion. *$p < 0.05$; *** $p < 0.001$ (One-way ANOVA followed by Dunnett's post test). C: EB3 comet alignment occurs at about 13 min. After 13 min, the rate of axon outgrowth increases and EB3 comets are aligned in the nascent axon (before 13 min, number of comets = 293; after 13 min, number of comets = 315). ***$p < 0.001$ (Student's t test). D: A kymograph constructed from a three pixel wide line drawn through the direction of axon extension. The kymograph line is linearized and compiled horizontally for each frame of the 30 min time lapse (601 frames). The arrow points to the initial alignment of EB3 comets. Arrowheads indicate protrusion from the growth cone. Scale bar: 5 μm.

nascent axon precedes persistent membrane protrusion. In three additional examples, reorientation of dynamic MTs in the direction of outgrowth also occurred prior to protrusion of a new axonal process from the growth cones, suggesting an instructive role for reorganization of dynamic MTs in spontaneous axon outgrowth.

Wnt5a Reorients and Redistributes Dynamic MTs in Growth Cones

Wnt5a accelerates cortical axon outgrowth (Li et al., 2009) in contrast to Wnt3a, which decreases DRG axon outgrowth while increasing growth cone size (Purro et al., 2008). The loss of directionality of dynamic MTs that moved across the growth cone rather than toward the leading edge was thought to lead to the eventual formation of MT loops characteristic of large pausing growth cones (Dent et al., 1999). Here, to determine the changes in the distribution and orientation of MTs during growth cone advance induced by Wnt5a, we imaged EB3 comets with TIRF microscopy in growth cones before and during bath application of Wnt5a. As shown in the fluorescence images [Fig. 3(A)], EB3 comets during 30 min before Wnt5a application explored all regions of the growth cone. EB3 comet tracks were overlaid onto DIC images of the growth cone and they show that MTs extend into filopodia in all directions without significant forward advance of the growth cone [arrows in Fig. 3(A)]. Using this technique, we also observed that under basal conditions, EB3 comets appear to target stable filopodia [arrows in Fig. 3(B)] more often than dynamic filopodia [arrowheads in Fig 3(B)]. Following Wnt5a application, EB3 comets repeatedly invaded fewer peripheral filopodia and invading comets were increasingly aligned in the direction of outgrowth along stabilized filopodia [Supporting Information Movie 2 and arrowheads in Fig. 3(A)]. Tracing of EB3 comet tracks in a representative growth cone before and during Wnt5a application showed that MTs became more bundled and aligned in the direction of axon outgrowth [Fig. 4(A), red-yellow colors indicates increased track overlap–see methods for details]. In each time-lapse movie, an average of 1272 EB3 comets were identified per 30 min period that comprised 262 $\pm$ 83 distinct comet tracks (averaging 4.9 $\pm$ 1.3 comets/track). EB3 comet tracks in each of six growth cones were traced over a 1-h period. A maximum image projection of total raw EB3 comets [Fig. 4(B)] and Gaussian curve fits of sum track pixel intensities across the entire growth cone [Fig. 4(C)] demonstrate the change in MT alignment. Decreases in the standard deviation of the Gaussian curve [Fig. 4(D,E)] demonstrate that MTs began to increasingly extend along similar pathways during Wnt5a treatment (p = 0.0313, Wilcoxon matched-pairs test). MTs reorganized from a splayed to a bundled array in these experiments. As previously seen, growth cones advanced faster in the presence of Wnt5a from an average of 1.2 $\pm$ 0.4 μm/h to 6.9 $\pm$ 2.0 μm/h (n = 5) during the 30 min treatment [Fig. 4(F)]. However, we found no consistent changes the velocity of EB3 comets or their track lengths. Strikingly, there was however a direct correlation between Wnt5a application and EB3 comet directionality, with faster outgrowth rates showing comet angles closer to zero (in the direction of outgrowth) [Fig. 4(G)].

MTs are thought to play a major role in orienting growth cones during turning behaviors (Buck and Zheng, 2002; Kalil and Dent, 2005). We asked whether repulsive cortical growth cone turning induced by Wnt5a (Li et al., 2009) is due to reorientation of dynamic MTs. Turning assays with Wnt5a gradients in TIRF microscopy proved to be impractical. However, we did capture spontaneous growth cone turning behaviors that could occur during bath application of Wnt5a. As shown in the example in Figure 4(H), before Wnt5a application EB3 comet tracks splayed out in all directions in the growth cone but during spontaneous turning EB3 comet tracks reoriented and bundled together in the direction of turning, similar to the reorientation of MTs in the direction of Wnt5a induced outgrowth. To determine whether MTs consistently redistribute in growth cones responding to Wnt5a gradients, we used a Dunn chamber assay (Yam et al., 2009; see Methods for details), in which Wnt5a was perfused across a bridge region between an inner and an outer chamber. Previously, we found with live cell imaging [(Hutchins and Kalil, 2011; and shown here in Fig. 6(C)] that cortical growth cones in the bridge region are repelled away from the direction of the Wnt5a gradient. After 2 h, the cultures were fixed and stained with antibodies to tyrosinated tubulin to label dynamic MTs (Brown et al., 1993; Dent and Kalil, 2001). As shown in Figure 4(I), dynamic MTs were redistributed to the far side of the growth cone facing away from the Wnt5a gradient. To compare MT distribution in Wnt5a versus BSA gradients, we measured fluorescence intensity of MTs in the far side versus the near side of the growth cone [Fig. 4(J)]. In the histograms values, above one indicate an asymmetry in which more dynamic MTs are distributed to the far versus the near side of the growth cone in Wnt5a gradients. In contrast growth cones in BSA showed no asymmetry in the distribution of dynamic

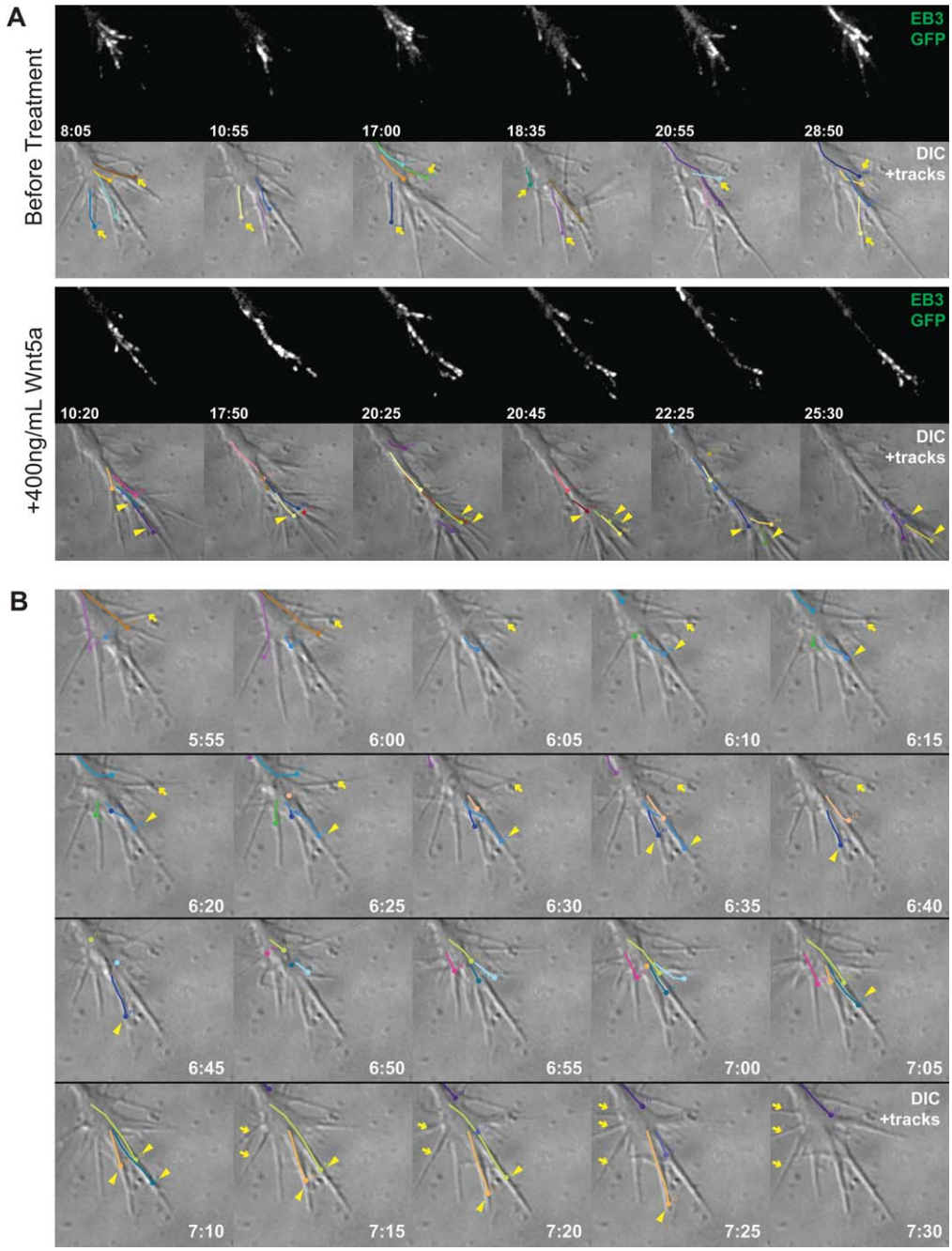

Figure 3 Dynamic MTs extend to stabilized filopodial tips that are aligned with the axis of Wnt5a-induced outgrowth. A: EGFP-EB3 transfected cortical neurons were imaged for 30 min prior to and 30 min after bath application with 400 ng/mL Wnt5a. The top panels for each condition are maximum projections of the raw EB3 comets over their lifespan (4–5 frames, ~20 s). EB3 comets were traced manually and comet tracks were overlaid onto DIC images that were acquired simultaneously (lower panels). Arrows indicate MTs extending randomly to filopodial tips throughout the growth cone before Wnt5a treatment. Arrowheads indicate MT tracks that become oriented along the axis of increased outgrowth during Wnt5a treatment. B: MTs invade filopodia that are more stable. Images of the same growth cone as in (A) before Wnt5a treatment showing each frame acquired over a 1 min 35 s period. Arrows indicate dynamic filopodia that are not invaded by MTs. Arrowheads show stable filopodia that are invaded by multiple MTs as indicated by EB3 comet tracks overlaid onto DIC images acquired simultaneously. Time is depicted in minute:second and each EB3 comet traced is represented by a different colored line showing the lifespan of the comet represented by the terminal dots in that frame.

MTs ($n = 26$ growth cones in Wnt5a and $n = 32$ growth cones in BSA). In shorter 30 min exposure periods in Dunn chambers (data not shown), Wnt5a gradients also induced a redistribution of dynamic MTs to the far side of the growth cone facing away from the Wnt5a gradient. These results suggest that as in spontaneous growth cone turning, dynamic MTs reorient in the direction of turning in response to a Wnt5a gradient.

Wnt5a Gradients Induce Asymmetric Calcium Activity in Growth Cones

Previous studies have shown that gradients of a guidance cue can evoke asymmetries in growth cone calcium activity (Henley and Poo, 2004; Gomez and Zheng, 2006) but higher levels of calcium have consistently been found on the side of the growth cone facing toward the source of the guidance cue, regardless of whether the cue is attractive or repulsive. Bath applied Wnt5a evokes repetitive calcium transients in cortical growth cones (Li et al., 2009). Here, we applied Wnt5a gradients through pipettes positioned 50 μm from growth cones that were up to 40 μm across, which permitted us to detect possible differences in calcium activity across the growth cone. Using the membrane bound calcium indicator Fluo4 MOMO to image calcium transients, we found that Wnt5a gradients could evoke global calcium activity throughout the growth cone as well as calcium transients localized to one side of the growth cone [Fig. 5(A,B)]. Out of a total of 39 growth cones 19 responded to Wnt5a with calcium activity and of these 14 (74%) showed asymmetrical calcium activity that was not localized to the region surrounding the midline. In growth cones expressing localized calcium activity 72% of the calcium transients were highest on the side of the growth cone facing away from the Wnt5a source [Fig. 4(C), $p < 0.005$, Wilcoxon signed rank test].

Tau Phosphorylated at Ser262 Is Required for Wnt5a Evoked Axon Outgrowth and Guidance

Since dynamic MTs and increased calcium transients were both asymmetrically distributed to the far side of the growth cone in Wnt5a gradients, we investigated their possible relationship. One candidate link is the MAP tau, which binds to MTs to increase their stability (Mandelkow et al., 1996; Dehmelt and Halpain, 2005). CaMKII, activated by calcium (Hudmon and Schulman, 2002; Lisman et al., 2002) has been shown to phosphorylate tau at the Ser262 MT binding site (Litersky et al., 1996; Sironi et al.,1998; Bennecib et al., 2001) leading to detachment of tau from MTs and decreased MT stability (Biernat et al., 1993). Moreover, Wnt5a can activate CaMKII (Kuhl et al., 2000), which, as we have shown, is required for Wnt5a induced axon outgrowth and repulsion (Li et al., 2009; Hutchins and Kalil, 2011), We therefore investigated tau as one possible link between calcium signaling and dynamic MTs.

Previous studies (Harada et al., 1994; Tint et al., 1998; Qiang et al., 2006) suggested that changes in levels of tau by itself might not be critical for regulating axon outgrowth. However, given the large number of tau phosphorylation sites (Shahani and Brandt, 2002; Johnson and Stoothoff, 2004) the selective phosphorylation of tau at the Ser262 MT-binding site by CaMKII (Sironi et al., 1998), and the critical role of phosphorylation at Ser262 for binding of tau to MTs *in vitro* (Biernat et al., 1993), we asked whether axon outgrowth and guidance by Wnt5a are regulated by tau Ser262 phosphorylation. We first immunostained cortical neurons with antibodies to tau phosphorylated at Ser262 and compared this with levels of total tau in axons and growth cones. As shown in the example in Figure 6(A,B), we compared average fluorescence intensities of phosphorylated tau versus total tau and expressed this as a ratio which was highest in the growth cone compared with the axon shaft. Bath application of Wnt5a, which increased rates of axon outgrowth from an average of 4.3–8.7 μm/h ($n = 27$ and 46 axons respectively), also increased the ratio of phosphorylated to total tau from 1.13 to 1.34 in these growth cones in comparison with BSA treated controls [Fig. 6(C–F)]. Moreover, faster axonal growth rates under all conditions ($n = 132$ axons) were positively correlated with higher ratios of phosphorylated to total tau [Fig. 6(F)]. Interestingly, smaller cortical growth cones that extend more rapidly than large growth cones (Halloran and Kalil, 1994; Szebenyi et al., 1998) had higher ratios of phosphorylated to total tau (data not shown). Taken together these results suggest that Wnt5a promoted axon outgrowth involves the phosphorylation of tau at Ser262 in the growth cone.

To determine whether the Ser262 tau-MT binding site is essential for Wnt5a evoked axon outgrowth and guidance, we transfected cortical neurons with a tau construct mutated at Ser262. As shown in the schematic [Fig. 7(F,G)], the mutated tau construct was made by substituting an alanine for serine to create a nonphosphorylatable site. The nonphosphorylatable tau S262A mutant protein acts as a dominant negative and would be unable to detach from MTs to increase their dynamics (Biernat et al., 1993). We

found that neurons transfected with tau S262A were unable to respond to bath applied Wnt5a with increased axon outgrowth (average axon length in Wnt5a+the control vector pcDNA3 = 386.5 ± 11.8 μm versus 242.9 ± 10.3 μm in Wnt5a + tau S262A) [Fig. 7(A,B)]. Transfection of tau S262A in control neurons exposed to BSA had no effect on axon length, which was similar to that of neurons transfected with the control vector pcDNA3 and treated with BSA. Next, we used Dunn chamber assays to determine whether tau phosphorylation at Ser262 is also required for Wnt5a evoked growth cone repulsion (Fig. 7). In Wnt5a gradients cortical axons increased their growth rates and showed repulsive turning [Fig. 7(D,E)]. However, in neurons transfected with tau S262A, axons failed to respond to

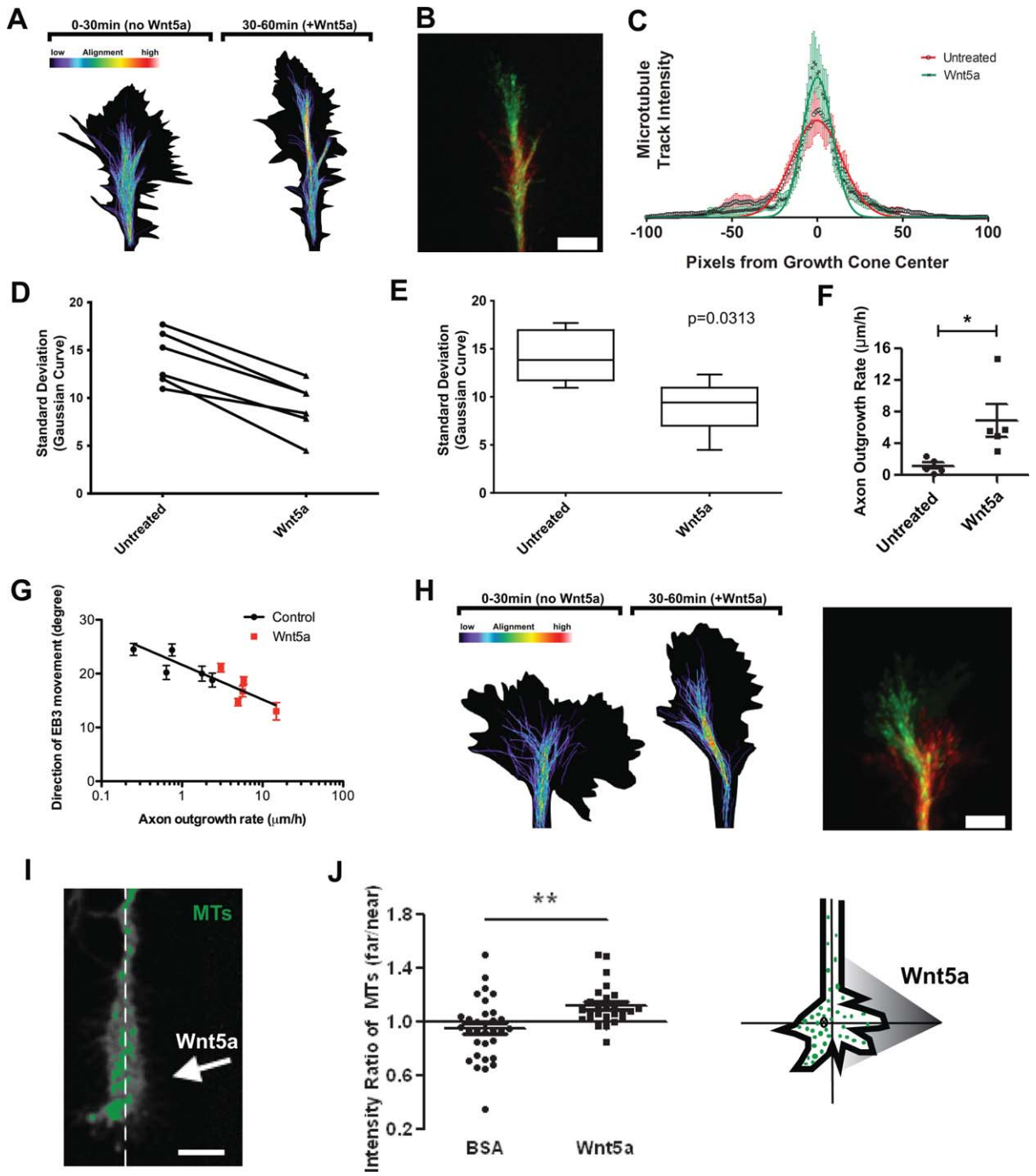

Figure 4 (See legend on following page.)

Wnt5a gradients and showed no increase in axon outgrowth (average axon outgrowth rates in Wnt5a = 13.0 ± 1.0 μm/h versus Wnt5a + tau S262A = 6.4 ± 0.4 μm/h) or repulsive turning [Fig. 7(C)] (average turning angles in Wnt5a = −18.6 ± 6.9° versus Wnt5a + tau S262A = 20.9 ± 12.9°. Taken together these results show that tau phosphorylation at the Ser262 MT binding site is necessary for Wnt5a evoked axon outgrowth and growth cone repulsion.

We hypothesized that the failure of cortical growth cones to respond to Wnt5a following mutation of tau at Ser262 was due to the inability of dynamic MTs to redistribute in the direction of axon outgrowth. We therefore imaged EB3 comets in growth cones (n = 6) of cortical neurons transfected with tau S262A. In neurons, transfected with a control pcDNA3 construct [Fig. 8(A)] growth cones responded to application of Wnt5a by increased advance together with changes in MTs from a splayed to a bundled organization similar to the untransfected neurons shown in Figure 4(A–E). In contrast, comet tracks traced in growth cones of neurons (n = 6) transfected with the mutated tau S262A showed that, concomitant with a lack of Wnt5a induced axon outgrowth, MTs remained splayed apart and failed to reorganize [Fig. 8(B)]. These results show that phosphorylation of tau at the Ser262 MT binding site is required for Wnt5a induced axon outgrowth mediated by the redistribution of dynamic MTs.

CaMKII Is Required for the Axon Outgrowth Effects of Wnt5a Mediated by Dynamic MTs

We have shown previously that CaMKII is required for the axon growth and guidance effects of Wnt5a in dissociated cortical neurons and in post-crossing callosal axons extending in cortical slices (Li et al., 2009; Hutchins and Kalil, 2011). CaMKII has been shown to be the major mammalian kinase to phosphorylate tau at Ser262 (Sironi et al., 1998; Bennecib et al., 2001) and we show that phosphorylation of this

Figure 4 Wnt5a induces redistribution and reorganization of dynamic MTs in growth cones. (A) Growth cones of EGFP-EB3 transfected cortical neurons were imaged for 30 min prior to and 30 min after bath application of Wnt5a as in Figure 3. EB3 comets were traced manually and all comet tracks overlain using a sum image projection and pseudocolored. Hotter colors indicate that MT tracks increasingly follow similar trajectories during Wnt5a treatment. Black outlines represent the extent of filopodial activity over each 30 min time period as determined by a maximum projection of DIC images acquired simultaneously, and show that the MT trajectories during Wnt5a treatment are in the direction of increased outgrowth. (B): Maximum image projection of raw EB3 comets from the entire 60 min movie in (A) with comets imaged before Wnt5a treatment colored red and comets imaged during Wnt5a treatment in green. (C) Line-scans 200 pixels wide across the geometric center of sum image projections of traced EB3 comet tracks in growth cones before (red) and during (green) Wnt5a treatment. Data are pooled from n = 6 growth cones and Gaussian curves have been fitted. D: Plot of the standard deviation from the Gaussian curve of each individual growth cone from the data in (C) before and after Wnt5a treatment. Lower standard deviations indicate more MT track overlap as measured by narrower, taller Gaussian curves. E: Sum of all standard deviations from (C, D). MT tracks are significantly more aligned during Wnt5a treatment. p = 0.0313 (Wilcoxon matched-pairs test). F: Axon outgrowth rates increase significantly with Wnt5a treatment. The velocity of five different growth cones (separate from A to E) was measured before and after bath application of Wnt5a in independent experiments. *p <0.05 (Student's t test). G: Wnt5a treatment is directly correlated with increased axon outgrowth rates. Directionality (degrees) of EB3 comets were assessed in the five growth cones analyzed in (F), and plotted against outgrowth rate (nonlinear regression, $p < 0.001$). H: Pseudocolored MT tracks and raw EB3 comets from a growth cone that spontaneously turned during Wnt5a bath treatment. MTs become aligned with the axis of the turn. I: Representative image showing immunostaining of tyrosinated tubulin in a fixed growth cone after exposure to a Wnt5a gradient in the Dunn chamber for 2 h. The top 50% of intensities are highlighted in green. Arrow indicates the direction of the Wnt5a gradient. The line indicates the midline of the growth cone as determined by the axon shaft. Scale bar: 10 μm. J: Quantitative analysis of MT asymmetry in growth cones exposed to Wnt5a gradients in the Dunn chambers. Bar graphs show the far/near ratios from growth cones under control (n = 32) and Wnt5a treatments (n = 26). A ratio above 1 indicates more MTs on the far side than on the near side and a ratio of 1 indicates no asymmetry. **$p < 0.01$ (Student's t test). A schematic of the measurement of the distribution of EB3 comets in the presence of a gradient of Wnt5a is shown.

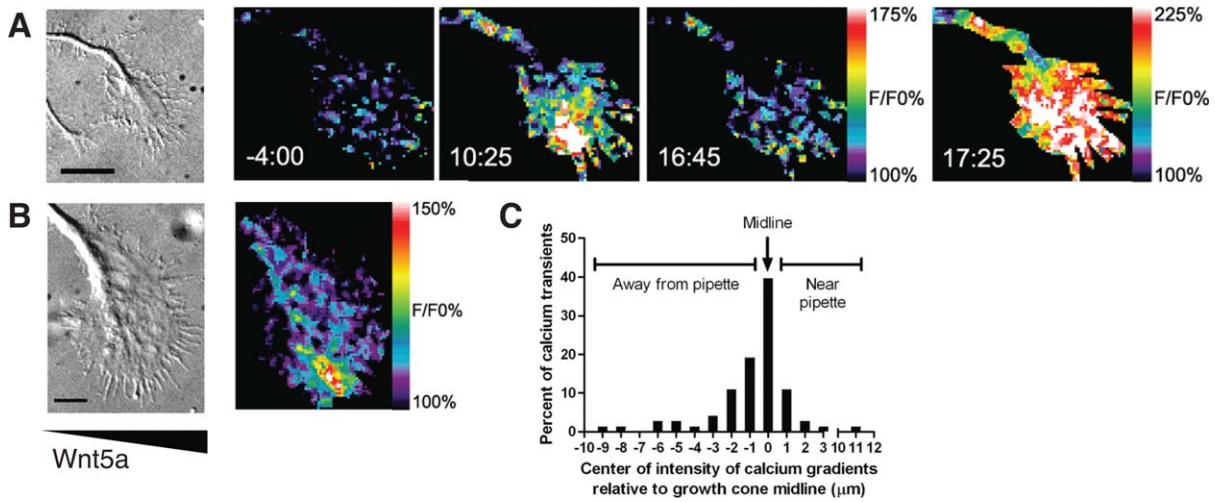

Figure 5 Wnt5a gradients induce asymmetric calcium activity in growth cones. A: Example of asymmetric local calcium activity at 10:25 evoked in the far side of the growth cone in a Wnt5a gradient applied to the right of the growth cone. A global calcium transient occurred at 17:45. Pseudocolor scale of fluorescence intensity is shown at right. An image of the same growth cone is shown at left in DIC. Scale bar: 10 μm. B: A second example of asymmetric local calcium activity evoked on the far side of the growth cone by application of a Wnt5a gradient. An image of the same growth cone is shown at left in DIC. Scale bar: 10 μm. C: Localization of the center of intensity of calcium transients evoked by application of Wnt5a gradients (n = 73 transients from 19 experiments). Negative numbers indicate localization of calcium transients to the side of the growth cone farthest from the pipette (center of intensity significantly different from 0, $p < 0.005$, Wilcoxon signed rank test).

tau MT binding site is essential for Wnt5a induced axon outgrowth through MT reorganization. However, since tau can also be phosphorylated at Ser262 by other kinases it was important to link CaMKII directly to effects on MT reorganization in growth cones exposed to Wnt5a. We therefore transfected cortical neurons with the specific CaMKII inhibitor construct EGFP-CaMKIIN. As shown in Figure 8(D), CaMKIIN expression prevents the reorganization of dynamic MTs in growth cones treated with Wnt5a (n = 8 growth cones). Tracing EB3 comet tracks showed that dynamic MTs failed to bundle during Wnt5a application, concomitant with the failure of Wnt5a to evoke axon outgrowth, and remained splayed apart in arrays similar to the growth cone before Wnt5a application [Fig. 8(C)]. These results link changes in MT organization mediated by phosphorylation of tau Ser262 to Wnt/calcium signaling through CaMKII.

DISCUSSION

The cytoskeletal mechanisms by which guidance cues evoke growth cone behaviors are not well understood (Dent et al., 2011). Meaningful correlation between cytoskeletal reorganization and growth cone behaviors requires high-resolution live cell imaging over time periods sufficient for guidance cues to evoke growth cone behaviors. This has been challenging for growth cones of mammalian CNS neurons. Here, we have accomplished this by using TIRF microscopy, which allowed high resolution imaging of the MT cytoskeleton for 1-h time periods, during which Wnt5a promotes cortical axon outgrowth and repulsive growth cone turning (Li et al., 2009). We demonstrate that Wnt5a evokes growth and guidance behaviors by reorganizing and redistributing dynamic MTs in the growth cone. Inhibiting MT dynamics with nocodazole or taxol prevented the axon outgrowth and repulsive guidance effects of Wnt5a. In live cell imaging during spontaneous axon outgrowth EGFP-EB3 comets aligned in growth cones in the direction of future axon outgrowth. Wnt5a increased axon outgrowth by reorganizing dynamic splayed MTs that explored all regions of the growth cone to bundled MTs that focused their extensions in the direction of axon outgrowth. In growth cones exposed to Wnt5a gradients dynamic MTs redistributed to the far side of the growth cone facing away

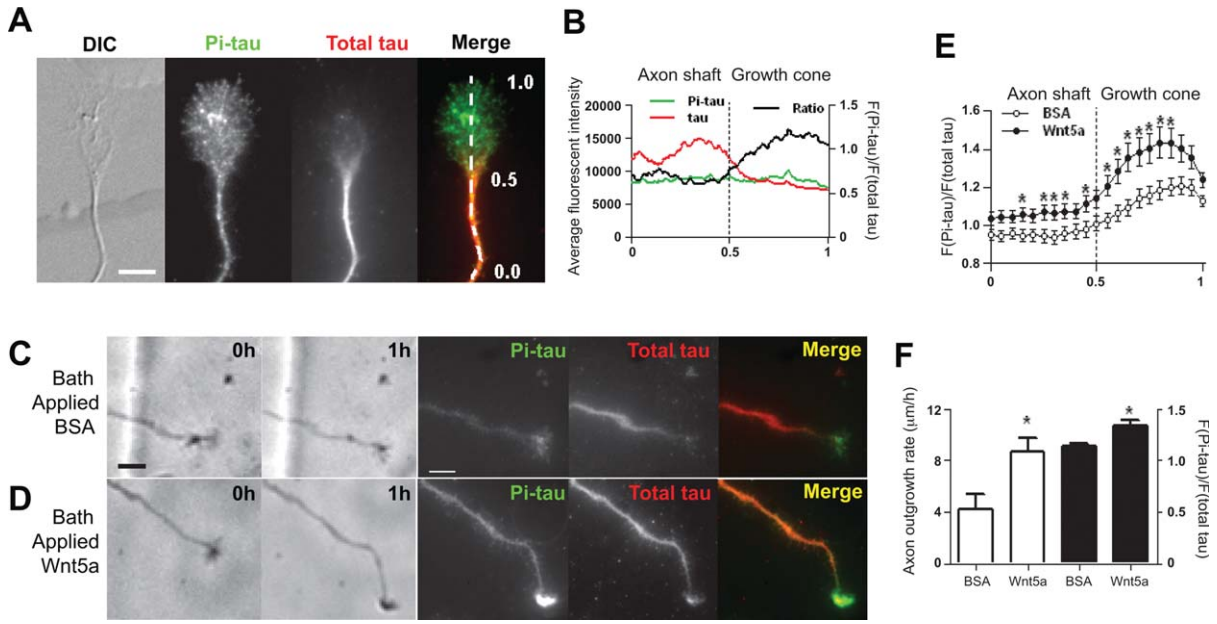

Figure 6 Phosphorylated tau (Pi-tau) at Ser262 is preferentially localized to the growth cone and increases relative to total tau in the presence of Wnt5a. A: Example of immunostaining showing the distribution of tau phosphorylated at Ser262 (Pi-tau in green) versus total tau (in red) in the growth cone and axon shaft. These distributions are quantified in (B). The axon and growth cone are shown in DIC at left. B: Fluorescence intensity of Pi-tau (green line) and total tau (red line) in the axon shaft (0.0 – 0.5 on the x axis) to the growth cone (0.5–1.0 on the x axis) of the neuron shown in A. Black lines show the ratio of Pi-tau over total tau from the axon shaft to the growth cone. Scale bar: 10 μm. C, D: Representative images of neurons treated with BSA or Wnt5a and then stained with anti-Pi-tau and total tau antibodies. At left are phase images of these neurons. Wnt5a applied in the bath for 1 h increases rates of axon outgrowth and the ratio of Pi-tau over total tau. Scale bar: 10 μm. E: Graphs showing the distribution of tau phosphorylated at Ser262 vs total tau from axon shafts to growth cones in BSA ($n = 27$) treated and Wnt5a ($n = 46$) treated neurons. In Wnt5a treated neurons, the ratio of Pi-tau versus total tau in axons and growth cones increased significantly. F: Bath applied Wnt5a ($n = 46$) increases ratios of Pi-tau over total tau compared with BSA (control, $n = 27$) and rates of axon outgrowth. In E and F, $^*p < 0.05$ (Student's t test).

from the Wnt5a source. This MT asymmetry coincided with higher levels of calcium transients on the far side of the growth cone in Wnt5a gradients, suggesting a link between calcium activity and dynamic MTs. We investigated the MAP tau as one possible link, and found that Wnt5a increased levels of phosphorylated tau relative to total tau, and that tau phosphorylated at Ser262, the MT binding site, is specifically required for Wnt5a induced axon outgrowth and repulsive guidance by mediating the reorganization of dynamic MTs. The finding that inhibition of CAMKII prevents Wnt5a evoked axon outgrowth by interfering with MT reorganization suggests a signaling pathway by which Wnt5a, through calcium signaling and tau phosphorylation, can influence the directionality of dynamic MTs in growth cones to elicit increased axon outgrowth and repulsive turning. These novel results for the first time link growth cone calcium activity directly to MT reorganization evoked by a guidance cue.

Guidance cues have been shown to have direct effects on MT organization and dynamics (Kalil and Dent, 2005). In Drosophila, Slit regulates midline axon crossing through Orbit/Mast. CLASP is the vertebrate ortholog of this MAP, which binds to the tips of dynamic MTs in Xenopus spinal neurons (Lee et al., 2004). Overexpression of CLASP causes the formation of MT loops to slow growth cone advance. Thus, the effects of guidance cues are mediated by changes in MT organization and dynamics through MAPs. Recently, Purro et al. (2008) found that Wnt3a regulates outgrowth of DRG axons by decreasing levels of the plus end MT binding protein APC and formation of MT loops, which increase

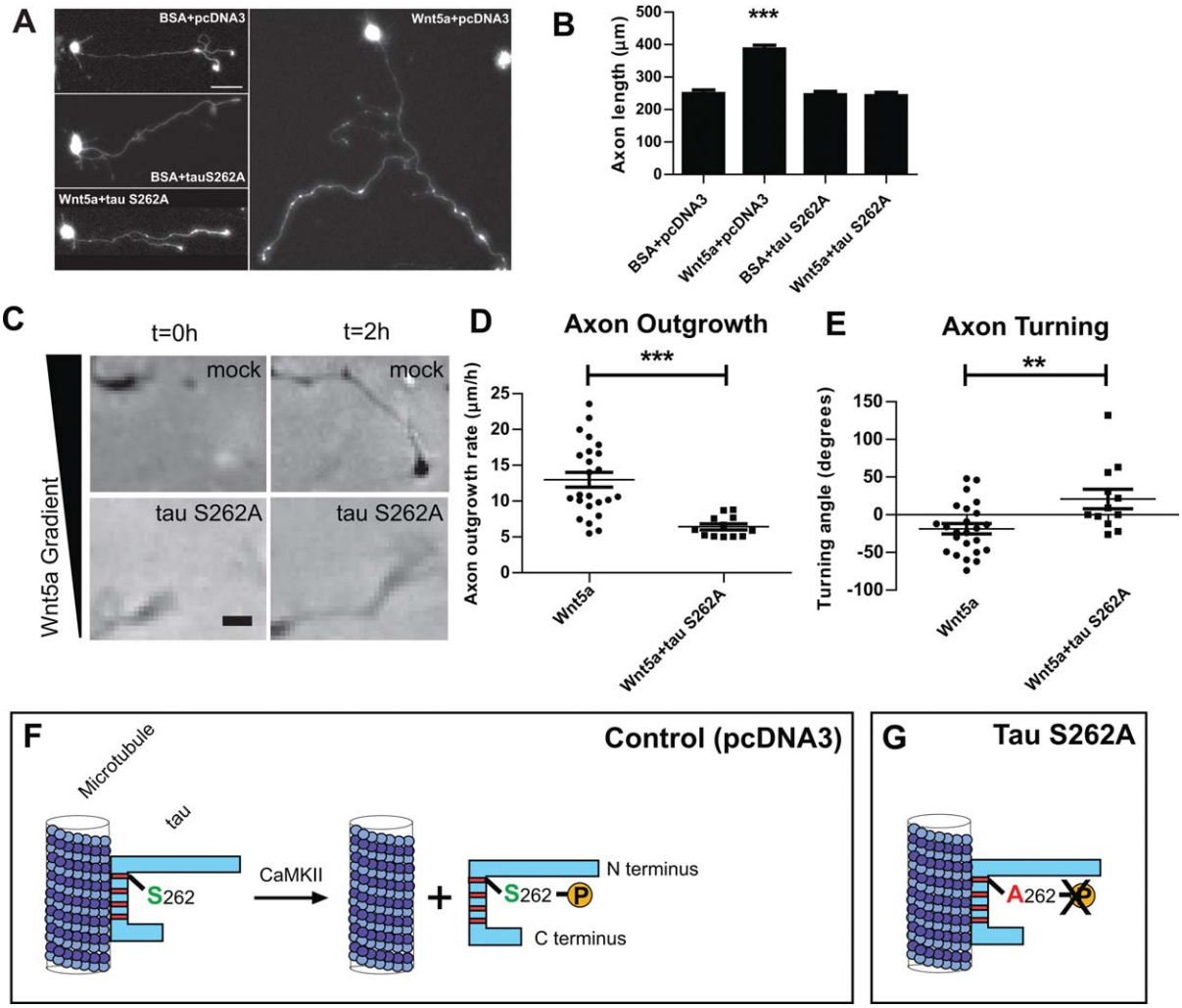

Figure 7 Phosphorylation of tau at Ser262 is required for Wnt5a-induced axon outgrowth and repulsion. A: Representative GFP fluorescence images of neurons in different conditions. Scale bar: 50 µm. B: Overexpression of tau S262A prevented increased axon outgrowth by Wnt5a. Quantitative analysis of axon length for the experiments shown in A. Mean and standard errors values are shown. ***$p < 0.001$ (One-way ANOVA followed by Dunnett's post test, $n > 60$ for each condition). C: Wnt5a gradients in the Dunn chambers failed to repel axons in neurons transfected with tau S262A. Examples of cortical axons at the beginning and end of 2 h exposure to Wnt5a gradients in Dunn chambers with or without tau S262A. Black bar to the left indicates the Wnt5a gradient decreased from top to bottom of the image. Scale bar = 5 µm. D, E: Inhibition of tau phosphorylation at Ser262 by transfection of tau S262A prevented Wnt5a induced axon outgrowth (D), and repulsive turning (E). ***$p < 0.001$; **$p < 0.01$, respectively (Mann-Whitney test, $n = 12$ for tau S262A, $n = 24$ for control treated). F, G: Schematic showing the attachment of tau to the MT at the S262 binding site (F). When CaMKII phosphorylates tau at this binding site, tau detaches form the MT (G).

growth cone size and decrease axon outgrowth. These results suggested that formation of stable MT loops was due to changes in directionality of dynamic MTs across the growth cone. In contrast, the growth promoting effect of NGF is mediated by a PI3K-GSK3β signaling pathway that regulates MT assembly by increasing rather than decreasing MT interactions with APC (Zhou et al., 2004). GSK3β diverges from the canonical Wnt/β-catenin pathway to regulate axon remodeling by the MT cytoskeleton (Ciani and Salinas, 2005), and has been implicated in the regulation of axon growth (Kim et al., 2006). Inhibition of GSK3β by Wnts (Budnik and Salinas, 2011) can inhibit axon outgrowth by decreasing MAP1B

phosphorylation and consequently stabilizing MTs into loops to stall growth cone advance. GSK3β can also phosphorylate tau (Johnson and Stoothoff, 2004; Stoothoff and Johnson, 2005; Brunden et al., 2009). Here, we show that the growth promoting effects of Wnt5a on cortical axons are opposite to the inhibitory

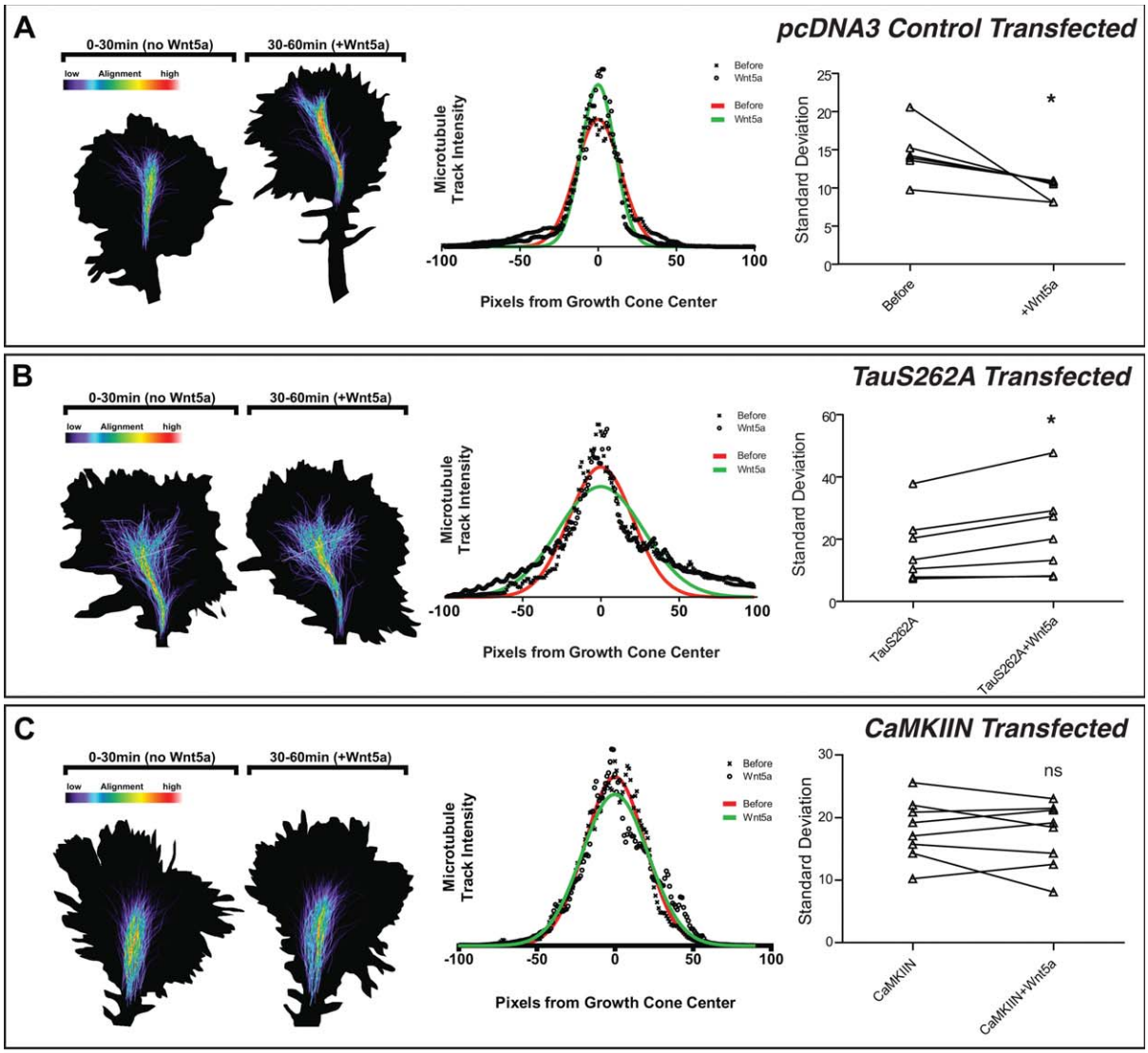

Figure 8

effects of Wnt3a on growth of DRG axons. In contrast to biasing MT directionality across the growth cone by Wnt3a (Purro et al., 2008), we show that Wnt5a changed the array of splayed MTs to a bundled organization such that dynamic MTs reoriented in the direction of increased axon outgrowth. Our findings suggest that tau phosphorylation at Ser262 occurs through calcium signaling involving CaMKII. Nevertheless, tau is only one possible link between calcium signaling and the redistribution of dynamic MTs. For example, changes in MT dynamics in growth cones can involve other components of calcium signaling pathways such as PKC (Kabir et al., 2001), which is also a component of Wnt/calcium signaling (Sheldahl et al., 1999). Moreover, tau has additional MT binding sites and numerous phosphorylation sites regulated by various kinases (Trinczek et al., 1995). Thus, although tau phosphorylation at Ser262 is highly effective in regulating the distribution of dynamic MTs in growth cones, this is only one mechanism for regulating dynamic MTs. Effects of Wnt5a on levels of GSK3β are unknown and effects of inhibiting GSK3β on axon outgrowth can be context dependent (Purro et al., 2008). However, it is possible that GSK3β might also contribute to tau phosphorylation and MT reorganization. Wnt5a could also increase axon outgrowth by regulation of APC at MT plus ends. Increased levels of APC have been correlated with increased neurite growth (Votin et al., 2005) and APC localizes to growth cones of extending neurites (Zhou et al., 2004). However, the role of APC in Wnt5a mediated axon outgrowth is unknown.

We have found that CaMKII is necessary for Wnt5a evoked growth and guidance of cortical axons in dissociated culture (Li et al., 2009) and in the corpus callosum in living cortical slices (Hutchins and Kalil, 2011). Moreover, CaMKII is one of the most effective kinases in the phosphorylation of tau at the Ser262 tau MT binding site (Sironi et al., 1998). *In vitro* phosphorylation of Ser262 alone is sufficient to attenuate the ability of tau to bind to MTs (Biernat et al., 1993) and detachment of tau from MTs leads to decreased MT stabilization. The involvement of calcium/CaMKII signaling in regulation of the MT cytoskeleton through tau phosphorylation is supported by our finding that inhibition of CaMKII prevents the MT reorganization underlying axon growth and guidance by Wnt5a. When we interfered with tau phosphorylation at the Ser262 site with a Ser262-Ala mutation, MTs were unable to reorganize in response to Wnt5a thereby preventing increased axon outgrowth. This raises the possibility that detachment of tau from MTs in growth cones is necessary for increased MT dynamics and their ability to reorganize to promote axon extension. Although this mechanism of MT regulation by tau phosphorylation has been documented *in vitro* (Biernat et al., 1993) a more recent study in Sf9 cells showed that tau phosphorylation of several sites including Ser262 within the MT binding domain were necessary for the outgrowth of neurite like cell extensions induced by transfection of wild type tau (Biernat and Mandelkow, 1999). These results are consistent with our findings in cortical neurons and suggest that increased MT dynamics by phosphorylation dependent detachment of tau from MTs underlies MT reorganization leading to axon outgrowth evoked by Wnt5a.

The mechanisms by which MT reorganization mediates axon outgrowth and guidance are not well understood. Our results suggest that MT bundling occurs before axon outgrowth and turning behaviors and is therefore an instructive rather than a

Figure 8 Tau phosphorylated at Ser 262, and CaMKII are required for Wnt5a induced axon outgrowth, and redistribution of dynamic MTs in growth cones. Cortical neurons were transfected with control pcDNA3 (A), TauS262A (B), or CaMKIIN-EGFP (C) plasmids along with EB3-tdTomato or EB3-GFP and imaged 30 min before and 30 min during Wnt5a bath application similar to Figure 3. A: Control pcDNA transfected cells showed an alignment of MT tracks along the axis of increased outgrowth similar to those in Figure 4 as indicated by "hotter" pseudocolored sum image projections of EB3 comet tracks, and lower standard deviations of Gaussian curves fitted from line-scans across the growth cones. $n = 6$ growth cones, $^*p < 0.05$ (Wilcoxon matched-pairs test). B: Inhibition of tau activity by transfecting cells with the mutant tauS262A construct prevented Wnt5a-induced outgrowth and MT tracks increased their "splayed" characteristics slightly as indicated by a slight increase in standard deviation. $n = 6$ growth cones, $^*p < 0.05$ (Wilcoxon matched-pairs test). C: Inhibition of CaMKII activity by transfecting cells with CaMKIIN-EGFP prevented Wnt5a-induced outgrowth and distribution of MTs remained random throughout the growth cone over the entire 60 min imaging period. D: Pooled data from standard deviations of Gaussian curve fits of EB3 comet track sum image projections in A–C.

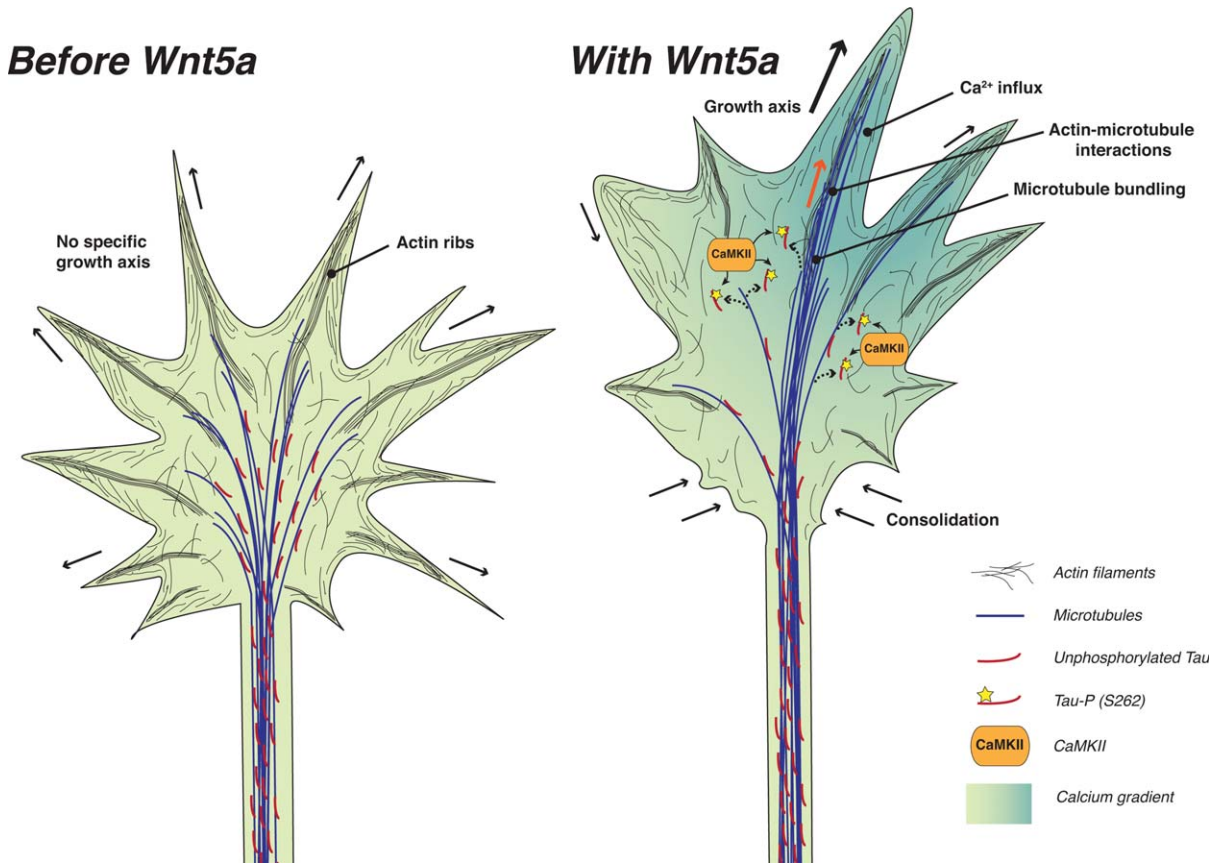

Figure 9 Model diagram showing the relationship between Wnt5a-induced calcium activity and MT reorganization during outgrowth. Before Wnt5a treatment (left), there is no polarization of increased outgrowth and the growth cone is free to move in any direction indicated by MTs randomly invading filopodia across the growth cone. During Wnt5a treatment (right), a calcium influx causes activation of CaMKII that in turn phosphorylates tau at S262, causing it to detach from MTs allowing them to reorient along an axis of increased outgrowth, possibly through interactions with each other and actin ribs along stabilized filopodia. As the growth cone realigns, unstable filopodia that are no longer visited by MTs are consolidated into the nascent axon.

permissive mechanism. Recent results have shown that the MT end-binding cytoplasmic linker proteins (CLIPs) are necessary for axon formation through their regulation of axonal MT stability and MT interactions with the actin network (Neukirchen and Bradke, 2011). In their model of axon outgrowth these authors proposed that neurite consolidation occurs by bundling of MTs in the growth cone center and that CLIPS, by stabilizing MTs, allow MTs to protrude into the growth cone tip and interact with the actin cytoskeleton. In contrast removal of CLIPs from MTs would prevent MT engorgement resulting in splayed MTs that increase growth cone size and axons that fail to extend. Our results are consistent with this model in that axon outgrowth requires bundling of MTs before consolidation of the trailing edges of the growth cone into an axon. As shown in our model (Fig. 9) one effect of Wnt5a is to promote MT alignment within stabilized filopodia, which are known to contain actin filaments bundled into ribs (Dent et al., 2011). Removal of tau from MTs might promote interactions with other MTs and with stable actin structures such as these. Since much of our understanding of the dynamic relationship between tau and MTs has been obtained from experiments using artificial cell-free systems, it will be important in future studies to investigate the conditions in which tau binds to and detaches from MTs in growth cones that are actively responding to environmental cues. It will also be important to determine whether tau regulates MT interactions with actin filaments during growth cone behaviors.

The authors thank Dr. Tim Gomez for the use of the TIRF microscope. They also thank Dr. Koichi Iijima and Dr. Kanae Iijima-Ando for the tau S262A constructs and Dr. Niels Galjart for the EGFP-EB3 construct, and Dr. Derrick McVicker for critical reading of the manuscript.

REFERENCES

Bennecib M, Gong CX, Grundke-Iqbal I, Iqbal K. 2001. Inhibition of PP-2A upregulates CaMKII in rat forebrain and induces hyperphosphorylation of tau at Ser 262/356. FEBS Lett 490:15–22.

Biernat J, Gustke N, Drewes G, Mandelkow EM, Mandelkow E. 1993. Phosphorylation of Ser262 strongly reduces binding of tau to microtubules: Distinction between PHF-like immunoreactivity and microtubule binding. Neuron 11:153–163.

Biernat J, Mandelkow EM. 1999. The development of cell processes induced by tau protein requires phosphorylation of serine 262 and 356 in the repeat domain and is inhibited by phosphorylation in the proline-rich domains. Mol Biol Cell 10:727–740.

Brown A, Li Y, Slaughter T, Black MM. 1993. Composite microtubules of the axon: Quantitative analysis of tyrosinated and acetylated tubulin along individual axonal microtubules. J Cell Sci 104 (Pt 2):339–352.

Brunden KR, Trojanowski JQ, Lee VM. 2009. Advances in tau-focused drug discovery for Alzheimer's disease and related tauopathies. Nat Rev Drug Discov 8:783–793.

Buck KB, Zheng JQ. 2002. Growth cone turning induced by direct local modification of microtubule dynamics. J Neurosci 22:9358–9367.

Budnik V, Salinas PC. 2011. Wnt signaling during synaptic development and plasticity. Curr Opin Neurobiol 21:151–159.

Ciani L, Krylova O, Smalley MJ, Dale TC, Salinas PC. 2004. A divergent canonical WNT signaling pathway regulates microtubule dynamics: Dishevelled signals locally to stabilize microtubules. J Cell Biol 164:243–253.

Ciani L, Salinas PC. 2005. WNTs in the vertebrate nervous system: from patterning to neuronal connectivity. Nat Rev Neurosci 6:351–362.

Clark CE, Nourse CC, Cooper HM. 2012. The tangled web of non-canonical Wnt signalling in neural migration. Neurosignals 20:202–220.

Dehmelt L, Halpain S. 2005. The MAP2/Tau family of microtubule-associated proteins. Genome Biol 6:204.

Dent EW, Callaway JL, Szebenyi G, Baas PW, Kalil K. 1999. Reorganization and movement of microtubules in axonal growth cones and developing interstitial branches. J Neurosci 19:8894–8908.

Dent EW, Gertler FB. 2003. Cytoskeletal dynamics and transport in growth cone motility and axon guidance. Neuron 40:209–227.

Dent EW, Gupton SL, Gertler FB. 2011. The growth cone cytoskeleton in axon outgrowth and guidance. Cold Spring Harb Perspect Biol 3.

Dent EW, Kalil K. 2001. Axon branching requires interactions between dynamic microtubules and actin filaments. J Neurosci 21:9757–9769.

Dent EW, Kalil K. 2003. Dynamic imaging of neuronal cytoskeleton. Methods Enzymol 361:390–407.

Gomez TM, Zheng JQ. 2006. The molecular basis for calcium-dependent axon pathfinding. Nat Rev Neurosci 7:115–125.

Govek EE, Newey SE, Van Aelst L. 2005. The role of the Rho GTPases in neuronal development. Genes Dev 19: 1–49.

Hall AC, Lucas FR, Salinas PC. 2000. Axonal remodeling and synaptic differentiation in the cerebellum is regulated by WNT-7a signaling. Cell 100:525–535.

Halloran MC, Kalil K. 1994. Dynamic behaviors of growth cones extending in the corpus callosum of living cortical brain slices observed with video microscopy. J Neurosci 14:2161–2177.

Harada A, Oguchi K, Okabe S, Kuno J, Terada S, Ohshima T, Sato-Yoshitake R, et al. 1994. Altered microtubule organization in small-calibre axons of mice lacking tau protein. Nature 369:488–491.

Henley J, Poo MM. 2004. Guiding neuronal growth cones using Ca2+ signals. Trends Cell Biol 14:320–330.

Huber AB, Kolodkin AL, Ginty DD, Cloutier JF. 2003. Signaling at the growth cone: Ligand-receptor complexes and the control of axon growth and guidance. Annu Rev Neurosci 26:509–563.

Hudmon A, Schulman H. 2002. Neuronal CA2+/calmodulin-dependent protein kinase II: The role of structure and autoregulation in cellular function. Annu Rev Biochem 71:473–510.

Hutchins BI, Kalil K. 2008. Differential outgrowth of axons and their branches is regulated by localized calcium transients. J Neurosci 28:143–153.

Hutchins BI, Kalil K. 2011. Wnt/calcium signaling mediates axon growth and guidance in the developing corpus callosum. Dev Neurobiol 71:269–83.

Johnson GV, Stoothoff WH. 2004. Tau phosphorylation in neuronal cell function and dysfunction. J Cell Sci 117: 5721–5729.

Kabir N, Schaefer AW, Nakhost A, Sossin WS, Forscher P. 2001. Protein kinase C activation promotes microtubule advance in neuronal growth cones by increasing average microtubule growth lifetimes. J Cell Biol 152:1033–1044.

Kalil K, Dent EW. 2005. Touch and go: guidance cues signal to the growth cone cytoskeleton. Curr Opin Neurobiol 15:521–526.

Keeble TR, Halford MM, Seaman C, Kee N, Macheda M, Anderson RB, Stacker SA, et al. 2006. The Wnt receptor Ryk is required for Wnt5a-mediated axon guidance on the contralateral side of the corpus callosum. J Neurosci 26:5840–5848.

Kim WY, Zhou FQ, Zhou J, Yokota Y, Wang YM, Yoshimura T, Kaibuchi K, et al. 2006. Essential roles for GSK-3s and GSK-3-primed substrates in neurotrophin-

induced and hippocampal axon growth. Neuron 52:981–996.

Krylova O, Herreros J, Cleverley KE, Ehler E, Henriquez JP, Hughes SM, Salinas PC. 2002. WNT-3, expressed by motoneurons, regulates terminal arborization of neurotrophin-3-responsive spinal sensory neurons. Neuron 35:1043–1056.

Krylova O, Messenger MJ, Salinas PC. 2000. Dishevelled-1 regulates microtubule stability: A new function mediated by glycogen synthase kinase-3beta. J Cell Biol 151: 83–94.

Kuhl M, Sheldahl LC, Malbon CC, Moon RT. 2000. Ca(2+)/calmodulin-dependent protein kinase II is stimulated by Wnt and Frizzled homologs and promotes ventral cell fates in Xenopus. J Biol Chem 275:12701–12711.

Lee H, Engel U, Rusch J, Scherrer S, Sheard K, Van Vactor D. 2004. The microtubule plus end tracking protein Orbit/MAST/CLASP acts downstream of the tyrosine kinase Abl in mediating axon guidance. Neuron 42:913–926.

Li L, Hutchins BI, Kalil K. 2009. Wnt5a induces simultaneous cortical axon outgrowth and repulsive axon guidance through distinct signaling mechanisms. J Neurosci 29: 5873–5883.

Lisman J, Schulman H, Cline H. 2002. The molecular basis of CaMKII function in synaptic and behavioural memory. Nat Rev Neurosci 3:175–190.

Litersky JM, Johnson GV, Jakes R, Goedert M, Lee M, Seubert P. 1996. Tau protein is phosphorylated by cyclic AMP-dependent protein kinase and calcium/calmodulin-dependent protein kinase II within its microtubule-binding domains at Ser-262 and Ser-356. Biochem J 316(Pt 2):655–660.

Liu Y, Shi J, Lu CC, Wang ZB, Lyuksyutova AI, Song XJ, Zou Y. 2005. Ryk-mediated Wnt repulsion regulates posterior-directed growth of corticospinal tract. Nat Neurosci 8:1151–1159.

Lohof AM, Quillan M, Dan Y, Poo MM. 1992. Asymmetric modulation of cytosolic cAMP activity induces growth cone turning. J Neurosci 12:1253–1261.

Lowery LA, Van Vactor D. 2009. The trip of the tip: Understanding the growth cone machinery. Nat Rev Mol Cell Biol 10:332–343.

Lucas FR, Salinas PC. 1997. WNT-7a induces axonal remodeling and increases synapsin I levels in cerebellar neurons. Dev Biol 192:31–44.

Luo L. 2002. Actin cytoskeleton regulation in neuronal morphogenesis and structural plasticity. Annu Rev Cell Dev Biol 18:601–635.

Mandelkow EM, Schweers O, Drewes G, Biernat J, Gustke N, Trinczek B, Mandelkow E. 1996. Structure, microtubule interactions, and phosphorylation of tau protein. Ann N Y Acad Sci 777:96–106.

Mikhailov A, Gundersen GG. 1998. Relationship between microtubule dynamics and lamellipodium formation revealed by direct imaging of microtubules in cells treated with nocodazole or taxol. Cell Motil Cytoskeleton 41:325–340.

Nakagawa H, Koyama K, Murata Y, Morito M, Akiyama T, Nakamura Y. 2000. EB3, a novel member of the EB1 family preferentially expressed in the central nervous system, binds to a CNS-specific APC homologue. Oncogene 19:210–216.

Neukirchen D, Bradke F. 2011. Cytoplasmic linker proteins regulate neuronal polarization through microtubule and growth cone dynamics. J Neurosci 31:1528–1538.

Norris CR, Kalil K. 1992. Development of callosal connections in the sensorimotor cortex of the hamster. J Comp Neurol 326:121–132.

Purro SA, Ciani L, Hoyos-Flight M, Stamatakou E, Siomou E, Salinas PC. 2008. Wnt regulates axon behavior through changes in microtubule growth directionality: A new role for adenomatous polyposis coli. J Neurosci 28: 8644–8654.

Qiang L, Yu W, Andreadis A, Luo M, Baas PW. 2006. Tau protects microtubules in the axon from severing by katanin. J Neurosci 26:3120–3129.

Reh T, Kalil K. 1981. Development of the pyramidal tract in the hamster. I. A light microscopic study. J Comp Neurol 200:55–67.

Salinas PC. 2012. Wnt signaling in the vertebrate central nervous system: from axon guidance to synaptic function. Cold Spring Harb Perspect Biol 4(2).

Salinas PC, Zou Y. 2008. Wnt signaling in neural circuit assembly. Annu Rev Neurosci 31:339–358.

Schaefer AW, Kabir N, Forscher P. 2002. Filopodia and actin arcs guide the assembly and transport of two populations of microtubules with unique dynamic parameters in neuronal growth cones. J Cell Biol 158:139–152.

Schaefer AW, Schoonderwoert VT, Ji L, Mederios N, Danuser G, Forscher P. 2008. Coordination of actin filament and microtubule dynamics during neurite outgrowth. Dev Cell 15:146–162.

Shahani N, Brandt R. 2002. Functions and malfunctions of the tau proteins. Cell Mol Life Sci 59:1668–1680.

Sheldahl LC, Park M, Malbon CC, Moon RT. 1999. Protein kinase C is differentially stimulated by Wnt and Frizzled homologs in a G-protein-dependent manner. Curr Biol 9: 695–698.

Sironi JJ, Yen SH, Gondal JA, Wu Q, Grundke-Iqbal I, Iqbal K. 1998. Ser-262 in human recombinant tau protein is a markedly more favorable site for phosphorylation by CaMKII than PKA or PhK. FEBS Lett 436:471–475.

Song HJ, Poo MM. 1999. Signal transduction underlying growth cone guidance by diffusible factors. Curr Opin Neurobiol 9:355–363.

Stepanova T, Slemmer J, Hoogenraad CC, Lansbergen G, Dortland B, De Zeeuw CI, Grosveld F, et al. 2003. Visualization of microtubule growth in cultured neurons via the use of EB3-GFP (end-binding protein 3-green fluorescent protein). J Neurosci 23:2655–2664.

Stoothoff WH, Johnson GV. 2005. Tau phosphorylation: physiological and pathological consequences. Biochim Biophys Acta 1739:280–297.

Szebenyi G, Callaway JL, Dent EW, Kalil K. 1998. Interstitial branches develop from active regions of the axon demarcated by the primary growth cone during pausing behaviors. J Neurosci 18:7930–7940.

Tanaka E, Ho T, Kirschner MW. 1995. The role of microtubule dynamics in growth cone motility and axonal growth. J Cell Biol 128:139–155.

Tanaka E, Kirschner MW. 1995. The role of microtubules in growth cone turning at substrate boundaries. J Cell Biol 128:127–137.

Tint I, Slaughter T, Fischer I, Black MM. 1998. Acute inactivation of tau has no effect on dynamics of microtubules in growing axons of cultured sympathetic neurons. J Neurosci 18:8660–8673.

Tojima T, Hines JH, Henley JR, Kamiguchi H. 2011. Second messengers and membrane trafficking direct and organize growth cone steering. Nat Rev Neurosci 12: 191–203.

Trinczek B, Biernat J, Baumann K, Mandelkow EM, Mandelkow E. 1995. Domains of tau protein, differential phosphorylation, and dynamic instability of microtubules. Mol Biol Cell 6:1887–1902.

Vasquez RJ, Howell B, Yvon AM, Wadsworth P, Cassimeris L. 1997. Nanomolar concentrations of nocodazole alter microtubule dynamic instability in vivo and in vitro. Mol Biol Cell 8:973–985.

Vitriol EA, Zheng JQ. 2012. Growth cone travel in space and time: the cellular ensemble of cytoskeleton, adhesion, and membrane. Neuron 73:1068–1081.

Votin V, Nelson WJ, Barth AI. 2005. Neurite outgrowth involves adenomatous polyposis coli protein and beta-catenin. J Cell Sci 118:5699–5708.

Wen Z, Zheng JQ. 2006. Directional guidance of nerve growth cones. Curr Opin Neurobiol 16:52–58.

Yam PT, Langlois SD, Morin S, Charron F. 2009. Sonic hedgehog guides axons through a noncanonical, Src-family-kinase-dependent signaling pathway. Neuron 62: 349–362.

Zheng JQ, Felder M, Connor JA, Poo MM. 1994. Turning of nerve growth cones induced by neurotransmitters. Nature 368:140–144.

Zheng JQ, Poo MM. 2007. Calcium signaling in neuronal motility. Annu Rev Cell Dev Biol 23:375–404.

Zhou FQ, Zhou J, Dedhar S, Wu YH, Snider WD. 2004. NGF-induced axon growth is mediated by localized inactivation of GSK-3beta and functions of the microtubule plus end binding protein APC. Neuron 42:897–912.